CHALLENGES IN EUROPEAN AEROSPACE
5TH CEAS AIR & SPACE CONFERENCE

CEAS

ANDROID Small Active Debris Removal Mission

Diego Escorial Olmos
GMV Aerospace and Defense S.A.U.
Project Manager, Systems Engineer
Isaac Newton, 11 P.T.M. Tres Cantos E-28760 Madrid, Spain
descorial@gmv.com

Thomas Vincent Peters
GMV Aerospace and Defense S.A.U.
GNC Engineer
Isaac Newton, 11 P.T.M. Tres Cantos E-28760 Madrid, Spain
tpeters@gmv.com

Joris Naudet
QinetiQ Space
Systems Engineer
Hogenakkerhoekstraat 9, 9150 Kruibeke, Belgium
joris.naudet@qinetiq.be

Cristian Corneliu Chitu
GMV Innovation Solutions S.R.L.
Systems Engineer
145 Victoriei St., Sector 1, 010072, Bucharest, Romania
cchitu@gmv.com

Karol Sewerin
Centrum Badań Kosmicznych Polskiej Akademii Nauk
Project Manager
ul. Bartycka 18a 00-716 Warszawa Poland
ksewerin@cbk.waw.pl

Tomasz Barciński
Centrum Badań Kosmicznych Polskiej Akademii Nauk
Project Engineer
ul. Bartycka 18a 00-716 Warszawa Poland
tbarcinski@cbk.waw.pl

ABSTRACT

Android mission is the result of an assessment study carried out by GMV under ESA contract with QinetiQ as subcontractor responsible for the platform design, CBK Poland responsible for the manipulator design and GMV Romania responsible for the net system design. The goal of the Android Mission is to demonstrate in orbit the critical technologies required for a future Active Debris Removal missions. The focus is set on the critical elements (GNC and capture mechanisms). The paper describes the system design performed during the activity.

1 ANDROID OVERVIEW

In recent years the concern about the future exploitation of space has been growing due to the risk that uncontrolled space debris poses to the space environment and therefore to the survivability of operational spacecraft. Two main regions of concern exist, GEO, where most of the commercial telecommunications satellites orbit, and LEO, where many scientific missions observing the Earth fly. Of special concern is the sun synchronous orbit, of special interest for Earth sciences. The population of debris in this region has been growing, increasing the risk of a collision and hence the exponential increase in the number of debris.
One of the possible solutions to this problem is Active Debris Removal (ADR). Recent studies show that the situation could be contained if 5 to 10 debris objects are removed per year. High mass objects posing a high risk of collision and hence debris proliferation should be removed first. These objects are usually large object with a large area and high energy, which in case of collision, would generate a big cloud of debris. In general, an ADR mission is a complex mission requiring the use of several novel technologies never tested in space before. The complexity of the mission also increases with the size of the target. Therefore in orbit demonstration of such technologies in a scaled down scenario is highly recommended. The goal of the ANDROID mission is to offer an affordable solution to test the technologies required for ADR mission. It will serve as a platform to test technologies and strategies required for other missions with different class targets. At this stage an investigation of the possible alternatives, technologies required and system level sizing have been carried out, paying attention to the most critical technologies, namely the guidance, navigation and control system and the capture mechanisms.
It is proposed to attempt at least two different capture techniques before the actual deorbiting of the target. The selection of the capturing techniques has been based on technology readiness level, generality and scalability criteria, resulting in the selection of a rigid method (robotic arm) and a flexible one (net system).The robotic arm capture will be performed first, followed by a set of secondary experiments and final capture with the net system to later deorbit the compound.

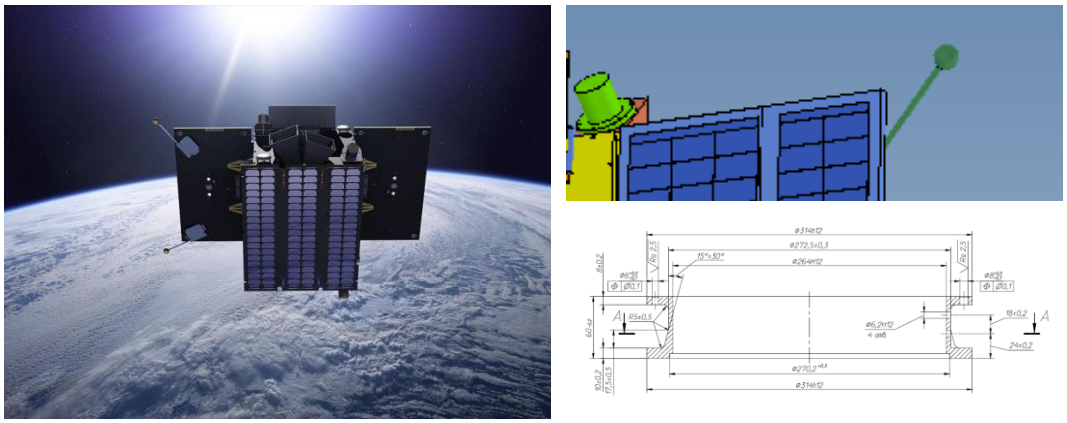

Figure 1: PROBA2 image and selected grasping points (adapter ring and DSLP antenna)

PROBA2 has been selected as target. PROBA2 was launched on the second of November 2009 by a Rockot launch vehicle. Currently it is still operational in a sun-synchronous orbit at 718km altitude with a local time of ascending node of 06h24 am. It has been assumed that by the time ANDROID is launched, PROBA2 is likely to be non-operational and considered as debris (though the ANDROID mission results could be boosted if it is still operational as it would retain its sensing and pointing capabilities). Initial analysis indicates that it should be spinning at an angular rate of 5 revolutions per orbit. Two grasping points have been identified; the adaptor ring (baseline) and the DSLP antenna as backup (TBC).

The mission is to be launched in a shared launch into LEO. The total mass of the system is expected to be under 350kg, with a total envelope with appendages of 1188(D)x1133(W)x1145(H)mm³. In terms of mass and dimensions there should be no problem in finding a candidate launch.
In terms of launch opportunities, SSO is a popular orbit for which several flights are done per year. The most popular orbits are around 650km altitude dawn dusk (quite close to the target orbit of Android) and 820km altitude 10:30 LTAN. A launch opportunity should be selected so that the ΔV and time required to arrive to the final orbit is minimised. Changes in inclination and RAAN can be extremely expensive in terms of propellant need and should be avoided. Initial assessment at this stage indicates that enough opportunities should exist in the coming years. Therefore the mission has been designed taking into account an allocation of ΔV for final orbit acquisition of 100m/s, which should cover the needs of almost any launch into a dawn dusk orbit.

2 MISSION ANALYSIS

Misison analysis yields a total ΔV requirement for the mission of about 400m/s (including margins). Table 1 below sumarises the mission phases, required time and ΔV. in terms of mission lifetime, one year will be enough to cover all the mission goals with confortable margins.

Table 1: ANDROID mission timeline and ΔV budget (without margins)

Phase	Time (h)	Time (h) w. margin	ΔV (m/s)
Orbit synchronization	9.91	2232	100.00
Commissioning	-		0
Rendezvous	25.79	108	6.33
Commissioning	56.18	236	10.18
Proximity Operations and Target inspection I	40.70	171	0.06
Additional experiments I	67.79	285	10.34
Robotic arm capture	9.61	40	0.02
Combo experiment	1.83	8	10.24
Target release	1.50	6	0.02
Additional experiments II	73.25	308	6.53
Proximity Operations and Target inspection II	30.44	128	0.05
Net capture	3.50	15	0.14
System stabilisation	1.65	7	0.01
Deorbit	11.26	47	182.30
Total	**333.43**	**3591**	**326.21**

The orbit synchronisation will be performed under ground control based on in-plane cotangential transfer manoeuvre and out-of-plane manoeuvres. Far rendez-vous will also be commanded from ground till the chaser is at a distance of about 2000 m behind the target and 500 m below. Subsequent phases will be carried out in an autonomous way under grond supervision for critial phases. The close rendez-vous will be based on a combination of drifting trajectories and safe orbit. Safe orbit will be extensively used throughout the misison, from rendez-vous to proximity operations including target inspection and robotic arm capture.
The safe orbit is characterised by a slight offset in the inclination and eccentricity vectors of the chaser orbit with respect to the one of the target. The resulting trajectory offers pasive safety, that is, if no actuation is performed there is no risk of collision between the two spacecraft. The trajectory can be seen as a circle centered in a point in V bar when projected in the ZY plane of the LVLH reference frame. The

characteistic dimension (diameter of the circle) and the location of the center on V bar can be freely selected depending on the use of the particular orbit.
The capture with the robotic arm will be performed from a safe orbit with the caser in free floating mode, while the capture with the net system will be performed from a hold point in V bar. Finally the deorbit burn will be performed through a series of impulsive manoeuvres aiming at direct controlled re-entry.

3 ADDITIONAL EXPERIMENTS

As part of the mission, additional experiments are also proposed. These experiments can be split into software experiments (mainly GNC systems and strategies) that will not require system modifications (only the use of resources like time and propellant) and hardware experiments, that will require some level of modification of the system to accommodate aditional payloads.
As part of the software experiments it is proposed to rehearse different strategies and GNC algorithms to perform spin synchronization with the target, which will be required in future ADR missions, especially when the target spin rate is high. Collision avoidance manoeuvres are also to be rehearsed. This functionality is part of the baseline mission, but if everything performs nominally they will not be executed during the mission, and in order to demonstrate them, they will have to be forced. Different strategies for the final rendez-vous can also be rehearsed, like hop rendez-vous, in which the chaser will approach the target by performing a series of hops along V bar.
As part of the mission it is also proposed to perform a deorbit exercise when the target is attached to the chaser via the robotic arm. Even though the final deorbit will be performed with the net system, the performance of the GNC system and the robotic arm itself should also be demonstrated. A short burn till steady state conditions are reached will be executed.
Finally it is also proposed to perform a demonstration of the COBRA concept. It relies on the use of chemical propulsion plume impingement on the target to change its dynamical status. It could be used for deorbiting small targets, but its main use will be to control the spin rate of the target though a contactless method. This functionality will be required in future missions where the target is spinning at a high rate to either reduce the rate or directly eliminate it. The chaser will fly around the target and fire the thruster pointing towards the target at the required rate so that the attitude can be controlled in closed loop.
As hardware experiments new sensors for ADR missions could be flown like flash LIDARs or infra-red cameras. Space components like in previous PROBA missions could also be a candidate as well as payloads of opportunity like space weather monitoring instrument.

4 SYSTEM DESIGN

The system is composed of a single spacecraft with a total wet mass of about 350kg including margins (see Table 2 below). Out of this mass 68 kg are propellant, about 20% of the launch mass. In case of larger propellant needs, the platform could be enlarged accommodating a larger hydrazine propellant tank. The main contributors to the mass of the system are the GNC equipment and the capture mechanisms comprising the robotic arm and the net system.

Table 2: ANDROID mass budget

Subsystem	Total mass [kg]	Mass margin [kg]	Total mass w margin [kg]
Structures	71.73	13.33	86.06
Thermal control	0.77	0.15	0.92
Communications	9.22	1.54	10.76
ADPMS	15.40	1.54	16.94

Subsystem	Total mass [kg]	Mass margin [kg]	Total mass w margin [kg]
GNC	34.02	3.11	37.13
Propulsion	17.66	2.19	19.85
Power	5.46	0.53	5.99
Harness	6.50	1.30	7.80
Capture systems	35.50	7.10	42.60
Total [kg]	196.26		228.05
System Margin (20%) [kg]			45.61
Total dry mass [kg]			**273.66**
Propellant mass [kg]			68.00
Total wet mass [kg]			**341.66**
Launcher IF ring [kg]			6.00
Total launch mass [kg]			**347.66**

4.1 Platform Design

The ANDROID spacecraft design is based on the PROBA-NEXT platform, which is the successor of the PROBA1, PROBA2 [1] and PROBA-V(egetation) [2] satellites developed by QinetiQ Space.
The PROBA-NEXT platform is a fully redundant all-purpose and generic platform that can host payloads in the range of 150kg and that can deliver more than 600W of power. It is a 3-axis stabilized platform providing a high pointing accuracy, with pointing errors below 30arcsec (95% confidence level). While the baseline configuration of the PROBA-NEXT platform offers upgraded downlink capacity (200Mbps) and mass memory storage (2Tbits) compared to the other members of the PROBA-family, it was decided to re-use the subsystems from PROBA-V, as they are in line with the requirements of the ANDROID mission.
The PROBA-NEXT platform has a 30 liter propulsion tank (23kg propellant) capacity, resulting in a delta-V of 200m/s for a typical 220kg S/C satellite. The ANDROID mission however calls for a significantly larger amount of propellant, as it needs to fully de-orbit the target satellite as well. This imposes the use of a propulsion tank with a volume of 90 liters. Therefore, the PROBA-NEXT platform structure was scaled up to fit the dimensions of the tank. The resulting total wet mass is about 275kg.

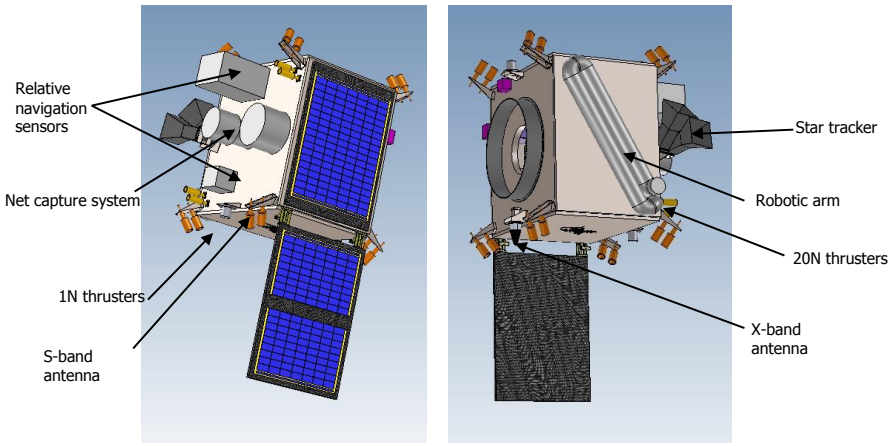

Figure 2: CAD model of the ANDROID spacecraft

The ANDROID spacecraft is shown in Figure 2, while Table 3 provides an overview of the different subsystems. On the left figure, the panel hosting the net capture system and the relative navigation sensors can be seen. On the right figure, the robotic arm is visible. The robotic arm has a relatively large

operating range that limits the possible configurations for the solar panels. A configuration with one body-mounted solar panel and one deployable panel was opted for, providing an average power of about 200W in a sun-synchronous dawn-dusk orbit.
The platform relies on star trackers for attitude determination and on reaction wheels for the attitude control. The relative position with respect to the target satellite is controlled by eight 1N thruster pairs located in the corners of the platform (pairs are used for redundancy), 20N thrusters are envisaged for large maneuvers such as orbit acquisition and de-orbit. A magnetic control loop based on magnetometers and magnetic torquers is used for the safe mode and for offloading the reaction wheel angular momentum.
For what concerns the communication subsystem, a S-band transceiver is accommodated for uplink of telecommands and downlink of the (low rate) platform telemetry, while a X-band transmitter is used for downlink of the (high rate) payload data.

Table 3: ANDROID platform subsystems

	ANDROID platform
Avionics	ADPMS (Advanced Data and Power Management System): Processor: LEON2-E (SPARC V8) Mass Memory Module : 11 GByte Interfaces: RS422, TTC-B-01, analogue and digital status lines, Packetwire, compact PCI
Power	Solar panels: 1 body-mounted and 1 deployable GaAs with 30% efficiency cells Battery: Li-ion, 28V, 12Ah Bus: 28V battery regulated voltage
Structure	Aluminium outer panels, Aluminium milled bottom board, CFRP outer panels with SA
AOCS	3-axis stabilised satellite Actuators: • 3 magnetic torquers (internally redundant) • 4 reaction wheels • 1N Hydrazine propulsion system • 20N Hydrazine propulsion system (deorbit) Sensors: • 2 magnetometers • 2 star trackers (with 2 camera head units) • 2 GPS receivers • 1 navigation camera • 1 inertial measurement unit • 3 sun sensors • 1 rendez-vous sensor (LIDAR)
Comms	S-band downlink: 827kbit/s and S-band uplink: 64ksps X-band downlink: 33Mbit/s
Software	Operating system: RTEMS Data handling/application software: based on PROBA-V OBSW
Thermal	Mainly passive thermal control, heaters for battery, propulsion subsystem and payload

4.2 GNC System Design

Preliminary design of the GNC system has been carried out defining all the necessary nominal and of nominal modes and transition as well as the required functionalities and performances in terms of guidance, navigation and control. The most critical phase for the system are the robotic arm capture phase followed by the deorbit burn.

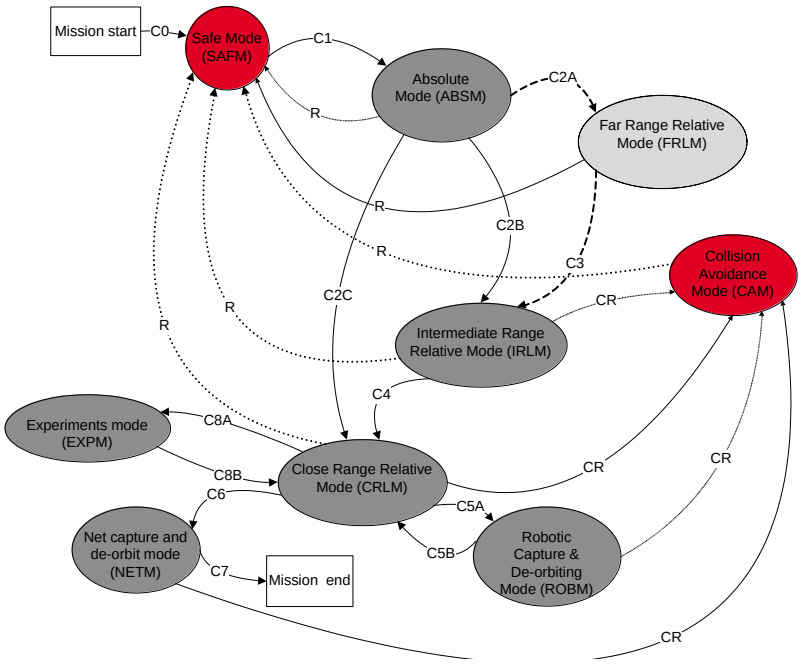

Figure 3: High-level GNC mode diagram

For the capture with the robotic arm a strategy based on a free floating platform has been selected. This approach leads to some simplifications at GNC level and at robotic arm control level and is perfectly applicable to the target considered. Should the spin rate of PROBA2 be higher than expected, a strategy based on spin synchronisation should be selected.

With respect to the GNC equipment selection, the main driver has been the TRL level. In order to keep the mission cost as low as possible, equipment with flight heritage has been selected, provided that the performance requirements are fulfilled.

In terms of actuators, apart from the magnetotorquers and reaction wheels, the main elements are the monopropellant thrusters. Two different set of requirements are imposed on this system, one for the proximity operations where high accuracy is required and a second for the main orbital manoeuvres (target orbit acquisition and deorbit burn). For the proximity operations a system composed of 16 1N thrusters is selected (redundant free torque and free force manoeuvres) with a minimum impulse bit of 2.6 mNs. For the orbital manoeuvres a system composed by for 20N thrusters (2+2 redundant) will be required to reduce the gravity losses. Furthermore this thruster will also have geometrical losses, as they will need to be de-pointed with respect to the deorbit burn direction so that the plume impingement on the tether is minimised.

The sensor system is composed of standard attitude control elements (star trackers, magnetometers, inertial measurement unit) plus the relative navigation sensors, composed of an optical camera and a LIDAR to support the proximity operations and provide robustness to the system to non optimal illumination conditions on the target. The cameras flown in the PRISMA mission (VBS from DTU Denmark and DVS from TDS Italy) would be perfect candidates for this mission. Performances would be better with the DVS, but performances achieved with the VBS should suffice once integrated with the LIDAR data. Accuracy provided will be enough from the initial range of 4km. From the LIDAR available technologies, a flash LIDAR would be preferred to a scanning LIDAR (lower disturbances and power demands in general), but unfortunately no flash LIDAR is available in Europe at the moment. Therefore it has been opted for the RVS developed by Jena Optronik and flown in ATV. It shall be noted that a new equipment

is under development (RVS3000) that could improve the performances of the mission (similar precision but lower mass, power and volume).
Three distinct simulators have been implemented to test three phases of the Android mission: close range rendezvous and target inspection, attitude synchronization and tethered stabilization and de-orbiting. The navigation function has not been included in any of the simulators and perfect navigation has been assumed. In reality the navigation will be based on camera and LIDAR measurements and it is expected that the accuracy of the navigation will be sufficient to perform each phase of the mission.
Close range rendezvous is the first completely autonomous phase of the mission. This phase will finish with the insertion of Android into a safe orbit, which is to be extensively used in ADR missions. The target inspection phase will be carried out from a drifting safe orbit. Figure 4 shows the guidance reference trajectory. The reference trajectory is generated as a maneuver plan, a sequence of maneuvers that takes the chaser from an initial drift orbit below and behind the target to a (inclination / eccentricity vector separated) safe orbit with a specific phase angle some distance behind the target. The phase angle and the distance of the safe orbit to the target are parameters of the plan generation.

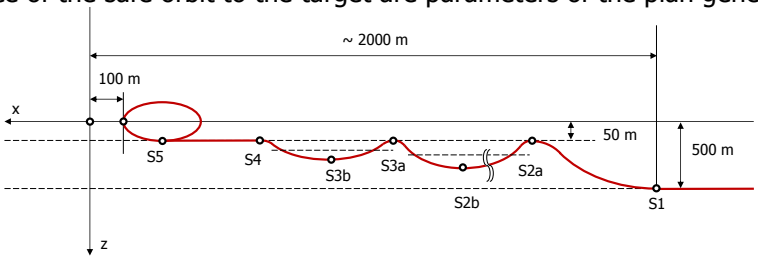

Figure 4: Guidance reference trajectory

The guidance function is composed of the plan generation function that provides a list of nominal maneuver times plus a reference trajectory and a two-point transfer maneuver computation function that is in charge of re-computing the nominal maneuvers and correction maneuvers occurring at fixed time intervals. Control during this phase is open-loop.
During the spin synchronization maneuver the chaser will perform a sequence of maneuvers to approach and synchronize itself with the target body fixed frame. The guidance function provides a reference profile in terms of position and attitude and feed-forward forces and torques to the control function. The control function is a simple LQR controller.

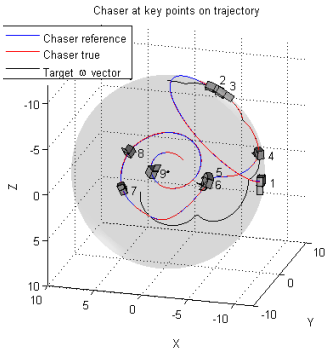

1-2: transition to rotation vector of target at 10 m distance
2-3: attitude synchronization with target using target body y-axis as reference
4-5: approach to target from 10 m to 5 m distance
6-7: transition to fixed on x-axis target body frame, maintaining attitude synchronization
8-9: approach to target from 5 m to 2 m

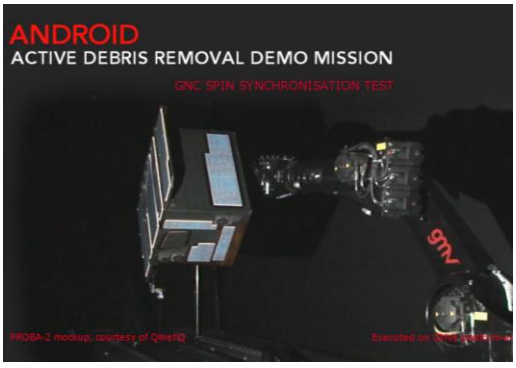

Figure 5: Android attitude synchronization (right) and platform-art test (left)

Figure 5 shows the elements of the guidance planning function. The synchronization plan features a series of fly-around at fixed distance, first to the projection of the target satellite's rotation vector and

then to an approach direction fixed in the target body frame. Straight-line approaches along these direction vectors are used. This scenario has been tested in *platform-art* (dynamic test bench) at GMV.
The third scenario simulates the tethered operations. Right after capture with the net the system will need to be stabilized, aligning the system with R bar. This may also be required during other phases of the mission, i.e. in between deorbit burns if there is a problem. The deorbiting of the target is the final goal of the mission. The system is composed by the chaser connected to the target via a flexible tether and subjected to a sequence of burns to lower the perigee. The guidance again consists of a plan generation function that provides a reference profile in terms of position and attitude and the forces and torques required to follow it. The reference profile takes into account the expected force transmitted by the tether. The two references profiles that are implemented are a fly-around to R-bar and the thrusting operations. As in the second simulator the control function is a simple LQR controller.

4.3 Net System Design

The conceptual design of the tethered-net system has been carried out aiming at determining the preliminary budgets associated with the proposed ADR scenario. Attention has been invested in analysing the scalability of such a system to larger targets. One main advantage of this technology is that it could be effectively applied to debris with various configurations and differences in characteristic dimensions. A generic tethered-net capturing system is considered to be composed of two main elements – net and tether – accompanied by the corresponding mechanisms: net folder/storage canister, bullet ejection mechanism, tether reel.
The proposed solution involves capturing the Proba 2 debris from a safety distance through the ejection of a tethered-net and by establishing a solid but flexible connection between the chaser and the target. The net deployment is performed by impulsively accelerating four corner weights (bullets) attached to the net mouth (perimeter ring). The bullets shall perform a dual role firstly by opening the net gradually (due to their momentum) in such a manner that the net is fully extended just before reaching the target debris and secondly by closing in and entangling on the target due to the same momentum. Additionally the use of two mechanisms (rotors) located in the bullets with the role of rolling in the cord that encompasses the net mouth shall assure the full closing of the net around the target. The net is linked to the tether through a central vertex (knot) which has the role of absorbing/distributing the loads. During net deployment the tether is left slack in order to reduce the interference on the dynamics of the net and avoid significant reaction forces on the chaser satellite. After the debris capture is successfully performed the tether is gradually tensioned and unwound in order to minimise longitudinal oscillations. A separation of 20 m between the two satellites has been selected for safety reasons resulting in a bullet divergence angle of 7° for firing the deployment bullets.

Net Design

Following a net configuration trade-off in terms of mass, manufacturing complexity and estimated deployment dynamics a planar design such as the one reported in [5] has been selected. It can be observed that the baseline configuration represents a hybrid between two planar configurations consisting of two types of elements with different thread diameters. This is because not all the net threads are active under non-symmetrical or tilted loading. From here, the idea of dividing net elements inside the net between working elements and containing elements: the working elements directly connected to bullets and tether with a diameter sized to withstand loads during shooting and de-orbiting phases; the containing elements with a smaller diameter and adapted to contain target hardware and withstand contact loads.
Subsequently a preliminary tool for estimating net properties has been developed to support the conceptual design work. The tool has been configured using the model described in [5] and adapted for the target debris order of magnitude. Based on the selected configuration the net size is computed using the debris characteristic length, at this stage solely determined by its maximum dimension. The worst

case scenario is considered in terms of shooting distance accuracy, chaser positioning, net deployment and entangling errors, thus yielding a net overlapping factor of 100%.

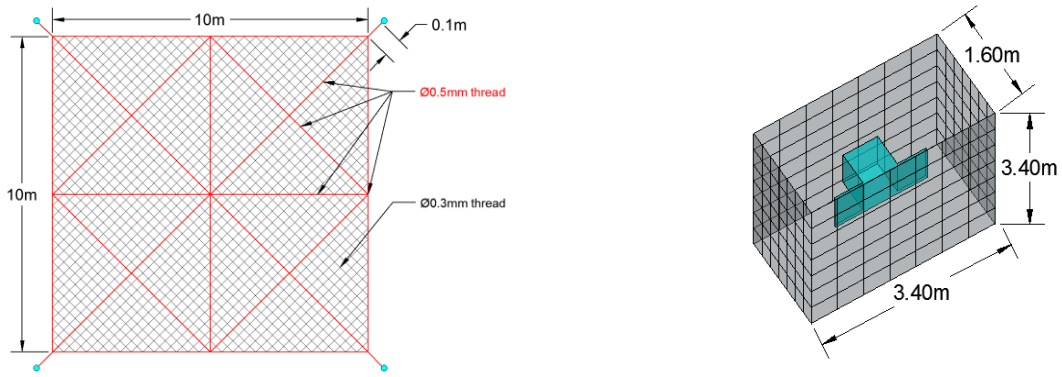

Figure 6: Proposed net configuration (left) and Total net envelope (right)

Additionally the selected net configuration yields a square mesh which is modelled with a selectable net/mesh dimension factor in the range [1%, 5%]. The netting type determines the total percentage of thread included in the knots, assumed at a value of 25%, yielding the required total net thread length. The maximum stress levels expected in the tether and net thread determine the minimum required cross-sectional areas. The selected planar configuration assumes equal sizing in diameters for tether and net diagonals and rings. For the remaining net thread the sizing accounts for all the four branches involved in a knot to evenly distribute the load, resulting in lower diameter requirements. Tuneable factors of safety (FoS) assumed in the estimation of the stress levels include a dynamic load factor of 4 (to be further iterated), general margin of safety (MoS) of 2, and optionally (TBC) a braiding FoS of 2, accounting for material properties degradation due to space environment conditions (UV exposure, atomic Oxygen). Net and tether mass is computed based on the materials density. The net deployment dynamic behaviour proposes a ratio between the net mass and the bullets total mass selectable in the range [1/6, 1/10]. The divergence angle and deployment time are computed based on the chaser – target shooting distance, net size and bullet ejection velocity. The change in ΔV is thus computed, accounting for the total ejected mass (only bullets effect), ejection velocity (considering instantaneous momentum transfer), divergence angle and chaser pre-deployment mass. Due to low ΔV computed magnitude no differentiation between spring driven and pressure fed net deployment mechanisms is accounted for at this level. The storage and deployment mechanisms have been inherited from ESA eDeorbit [4] and scaled down where considered necessary (net container). The mechanisms sizing is verified against the volumetric requirements estimated with the proposed folding factors, 5x for net and 2x for tether spool.

Table 4: Net System Budget

Component	Mass [kg]	Volume [cm^3]	Diameter [m]	Length [m]
Net (incl bullets)	1.45	1000	0.0003/0.0005 (10)	10
Tether (incl center knot)	0.1	100	0.0005	200
Storage Cannister + Net ejector	6.1	4710	0.2	0.15
Reel	5.5	3000	0.16	0.15
TOTAL	13.15	8000	0.2	0.3
TOTAL (20% Margin)	15.8	10000	-	-

Tether

The tether diameter has been determined using the worst case scenario in terms of tensile stress occurring during the de-obiting phase when the tether is stretched. As a first estimation, a 200m long tether was considered in this study, manufactured from braided yarns of Dyneema. The factors of safety considered in the analysis are the same as in the net dimensioning case. The analysis yields a minimum required diameter of 0.5mm resulting in a total mass of aprox. 100g and a required storage volume of aprox. 100cm3. An extra factor of safety of 2 is suggested here, raising the minimum tether diameter to 1.1mm, to account for material properties degradation.

The first 20m close to the chaser satellite have been treated separately due to the effects of thrusters' plume impingements. To this end, Carbon Fiber T1000G has been proposed as core material for this tether segment. The link between the two segments may constitute an important challenge. The proposed solution is an intercalated yarn braiding between the two different cores on a length that would assure the yarn to yarn friction necessary to keep the integrity of the tether. As a second solution, a CF jacket can be woven around the Dyneema core for the mentioned tether segment, acting as an insulation material.

Materials

As output of the preliminary analysis, Dyneema®SK75 produced by DSM High Performance Fibers in The Netherlands has been selected as preferred candidate for manufacturing both the tether and the net thread. Dyneema is an ultra-high molecular weight polyethylene with characteristics that make it suitable for the mission in discussion. It can be produced in uninterrupted filaments of 12-21 μm, having one of the highest specific strengths achieved in commercial fibres with a low volumetric density. Additionally it has a friction coefficient of just 0.06 and a fatigue resistance 10 times better than the p-aramids. Having a low absorption coefficient $\alpha=0.2$ and high emissivity of $\varepsilon=0.8$ it is suitable for space applications, becoming brittle only at -150. One major disadvantage of these fibres is the degradation of strength with temperature, starting at just 70°C, with the melting point at around 150°C. Reduction factors for the degradation of strength and modulus due to temperature, UV influence and knotting were proposed in the thread diameter sizing using a safety factor of 2.

4.4 Robotic Arm design

Modelling, simulation and path planning of free floating mode

In point of view dynamical systems theory, the manipulator mounted on the satellite and operating in on orbit environment is a nonlinear, time-varying, infinite-dimensional system. In fact, the manipulator is consisted of a couple of jointed beams, and each beam is subjected to wave effects, therefore its state is infinite-dimensional vector. Similar model concerns of the satellite with elastic panels. The forces, torques, velocities and other state variables and signals in the system are related with nonlinear equations, which originate from the system geometry, mass distribution and principles of conservations. Moreover, the gravitional gradient and orbital non-inertial forces act on the system. High precision mathematical model taking into account all of the abovementioned elements would be extremely hard for performing analysis based manipulator design and path planning, therefore it shall be simplified.

In the first approximation we make the following assumptions:

1) Satellite is rigid body;
2) Links of the manipulator are rigid bodies;
3) Friction in joints is linear;
4) Joints are directly driven (without gear) by electrical motors;
5) Non-inertial forces are neglected;
6) Gravitational gradient is neglected.

With assumptions 1-6 the mathematical model can be formulated with General Jacobian Matrix (GJM) approach introduced by Umetani and Yoshida [9] and extended by Seweryn for systems in which linear and angular momentum are not conserved [10, 11]. The starting point of modelling the satellite mounted manipulator in free floating mode is the principle of momentum conservation, which has the following form

$$(J_M - J_S H_2^{-1} H_3)\dot{q} = \begin{bmatrix} v_{ee} \\ \omega_{ee} \end{bmatrix}, \tag{1}$$

where J_M, J_S are the Jacobian of the manipulator and the satellite, respectively, $\dot{q}$ is configurational velocity of the manipulator, v_{ee} and ω_{ee} are linear and angular velocity of the end effector, respectively. Matrices H2and H3 contains dynamic coupling between the manipulator and the satellite:

$$H_2(q, r_s) = \begin{bmatrix} (m_s + \sum_{i=1}^{n} m_i) I & (m_s + \sum_{i=1}^{n} m_i)\tilde{r}_{s\_g} \\ \left((m_s + \sum_{i=1}^{n} m_i)\tilde{r}_{s\_g}\right)^T & I_s + \sum_{i=1}^{n}\left(I_i + m_i \tilde{r}_{i\_s}^T \tilde{r}_{i\_s}\right) \end{bmatrix} \tag{2}$$

$$H_3(q, r_s) = \begin{bmatrix} \sum_{i=1}^{n} m_i J_{Ti} \\ F \sum_{i=1}^{n}\left(I_i J_{Ri} + m_i \tilde{r}_{i\_s}^T J_{Ti}\right) \end{bmatrix} \tag{3}$$

where

$r_{s\_g} = r_s - r_g$

$r_{i\_s} = r_i - r_s$,

In the above equations $r_s$is the position of the satellite centre of gravity, r_g is the position of the manipulator mounting point with respect to satellite centre of gravity, r_i is the position of i-th kinematic pair of the manipulator, $m_s$is the mass of the satellite, m_i is the mass of i-th manipulator link, I is the identity matrix, $I_i$is the inertia matrix of i-th manipulator link, $I_s$is the inertia matrix of the satellite, J_{Ti} is the translational component of manipulator Jacobian (expressed in inertial Coordinate System), and J_{Ri} is the rotational component of this Jacobian.

The system (1)-(3) is self-contained dynamical system, which can be solved with respect of manipulator configuration q, when end effector velocity is given as a function of time. Therefore it can be used for end-effector trajectory planning. In the Figure 7 it is presented exemplary solution to the system (1)-(3) where the end-effector velocity is leading the end-effector towards a selected point.

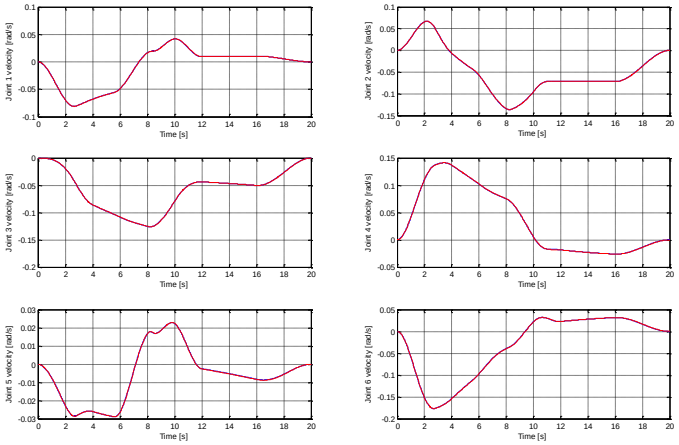

Figure 7: 6DOF Manipulator configurational velocities during free floating operation

Forces and torques Q acting within the system are described by

$$M(q)\ddot{q} + C(\dot{q}, q)\dot{q} = Q \tag{4}$$

Where

$$M(q) = N + H_3^T H_2^{-1} H_3 \tag{5}$$

$$N = \sum_{k=1}^{n} \left(\frac{\partial m_{ij}}{\partial q_k} - \frac{1}{2} \frac{\partial m_{jk}}{\partial q_i} \right) \dot{q}_k \quad , \quad M(q) = [m_{ij}] \tag{6}$$

The system (1)-(3) together with (4)-(6) forms full mathematical model of the free floating manipulator mounted on satellite. It is worth noting that the dynamic part of the system can be solved sequentially, i.e. the system (1)-(3) does not depend on the latter part (4)-(6). Hence, the analysis of movement – kinematics can be performed on the relatively simple model. For more examples refer to [12].

Manipulator Design

The length of the manipulator is basically determined by the distance from the target which shall be captured by the end-effector. In the case considered in this paper the sphere contained the rotating object to be captured has radius about 1.9 meters. The manipulator shall reach any point on the target, the distance between the innermost point on the target and the boundary sphere is about 1.5 meters. Moreover, safety margin shall be taken into account, thus in this case we assumed 20% which gives us about 0.3 meters. Therefore, the overall length of the manipulator shall exceed 3 meters.

From various types of manipulators we choose an architecture which originates in the anatomy and functionality of human elbow. This architecture has an extensive heritage in on-Earth applications.

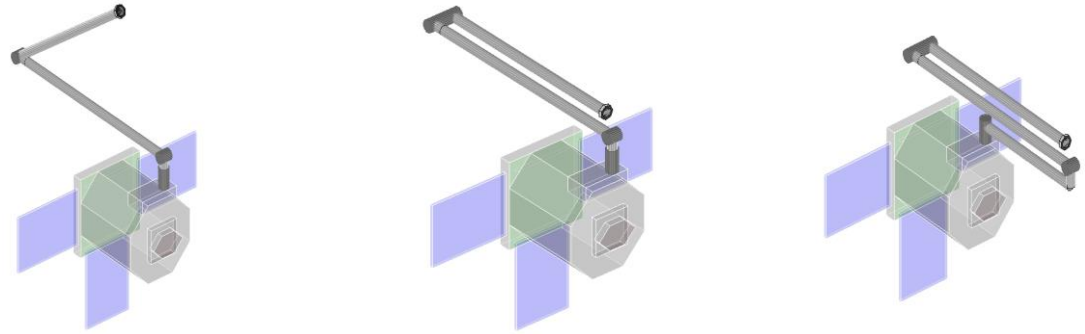

a) **b)** **c)**

Figure 8: Manipulator configuration selection

The architecture is presented in the Figure 8, in three variants of different folding ability: a) anthropomorphic with links in common plane (thus it cannot be folded), b) anthropomorphic with folding ability, links are placed in two parallel planes, c) compact with second joint offset. The manipulator will operate in plane (Figure 9).

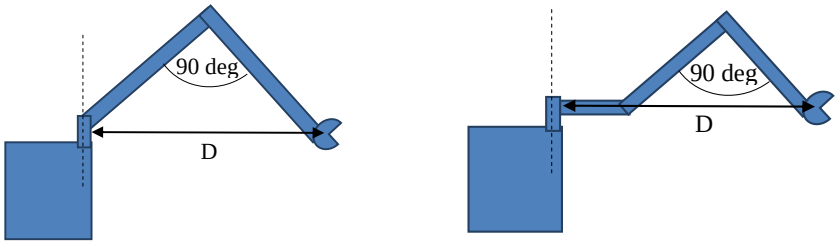

Figure 9: Operation plane, conf. a) on the left, conf. b) on the right

The anthropomorphic case (b) and compact case (a) has maximal manipulability around third joint position of 90 deg, therefore the manipulator has largest range D from the mounting point with the largest manipulability when it has the pose presented in the Figure 9. Although the compact manipulator has worse manipulability properties than the anthropomorphic in general, in considered case when it operates around the plane, both of manipulator architecture has similar properties. The compact manipulator is more feasible in considered space mission because it occupies less space when it is folded. The main components of the robotic arm (joints) could be based on already existing hardware or already under development like the manipulator prototype under development in Centrum Badań Kosmicznych PAN, Poland or the ones developed for ESA, DexArm. The envisaged mass for the system is 18kg.

5 CONCLUSIONS

Preliminary design for an affordable and feasible mission for active debris removal in orbit demonstration has been carried out and presented in this paper. The mission will target PROBA2 and will demonstrate GNC technologies together with a rigid capture mechanism (robotic arm) and a flexible one (net system). The design is based mostly on existing technologies, and development plans have been analysed for the new technologies during the course of the study. The required development time would be under 2 years, making it feasible to launch a mission of these characteristics in the coming 2-4 years if the programmatic framework is put in place.

6 REFERENCES

[1] D. Gerrits, J. Naudet, S. Ilsen, S. Santandrea et al., PROBA-2: over four years of autonomy, technology demonstration, solar science and space weather monitoring, 4S Symposium, Spain, 2014.
[2] J. Dries, S. Sterckx, I. Benhadj, T. Van Roey, PROBA-V in-flight results, one year after launch, 4S Symposium, Spain, 2014.
[3] PATENDER - Net Parametric Characterisation and Parabolic test, GMV proposal to ESA ITT Reference AO 1-7452/13/NL/RA
[4] R. Biesbroek, The e.Deorbit CDF Study Report CDF-135(C)
[5] R. Benvenuto, R. Carta, A. Bombelli, M. Lvagna, R. Armellin, Experimental Set-up of a Net-Shaped Space Debris Removal System,
[6] R. Benvenuto, R. Carta: Active debris removal system based on tethered-nets: experimental results, Aerospace Science and Technology Dept., Politecnico di Milano, Via La Masa 34, 20156 Milano, Italy; in Proc. of 9th Pegasus-AIAA Student Conference, Politecnico di Milano, Italy, 2013
[7] Bombelli A., Benvenuto R., Carta R., Lavagna M., and Armellin R. Optimal Design of a net-shaped space debris removal system. In Proc. 5th ICATT, ESA-ESTEC
[8] Michiel Kruijff, Tethers in Space. A propelantless propulsion in-orbit demonstration, PhD thesis at TU Delft, Faculty of Aerospace Engineering, 2011
[9] Umetani Y., Yoshida K., "Resolved motion rate control of space manipulators with Generalized Jacobian Matrix." IEEE Transactions on Robotics and Automation, Vol.5, No.3, 1989.
[10] Seweryn K., "The dynamics of the satellite rendezvous and docking maneuver using nonholonomic robotic arm," Ph.D. Thesis, Faculty of Power and Aeronautical Engineering, Warsaw University of Technology, Warsaw, 2008.
[11] Seweryn K. and Banaszkiewicz M., "Optimization of the trajectory of a general free - flying manipulator during the rendezvous maneuver," in Proc. of the AIAA Guidance, Navigation and Control Conference and Exhibit. Honolulu, Hawaii, USA, 2008.
[12] Rybus, T., Lisowski, J.,Seweryn, K., and Barcinski, T., Numerical simulations and analytical analyses of the orbital capture manoeuvre as a part of the manipulator-equipped servicing satellite design